

# Study of the phase transition and charge ordering in single-crystalline $\text{Nd}_{1/2}\text{Sr}_{1/2}\text{MnO}_3$ using x-ray scattering

C.-H. Du,<sup>1,a)</sup> M. E. Ghazi,<sup>2,b)</sup> P. D. Hatton,<sup>2</sup> S. P. Collins,<sup>3</sup> B. M. Murphy,<sup>4</sup> B. G. Kim,<sup>5</sup> and S.-W. Cheong<sup>5</sup>

<sup>1</sup>Department of Physics, Tamkang University, Tamsui 251, Taiwan

<sup>2</sup>Department of Physics, University of Durham, Durham DH1 3LE, United Kingdom

<sup>3</sup>Diamond Light Source Ltd., Rutherford Appleton Laboratory, Chilton, Didcot, Oxon OX11 0QX, United Kingdom

<sup>4</sup>Institut für Experimentelle und Angewandte Physik, Universität Kiel, Germany

<sup>5</sup>Rutgers Center for Emergent Materials and Department of Physics & Astronomy, Rutgers University, New Jersey 08854, USA

(Received 8 March 2008; accepted 16 May 2008; published online 21 July 2008)

We report a sequent phase transition using high-resolution synchrotron x-ray scattering in a single crystal  $\text{Nd}_{1/2}\text{Sr}_{1/2}\text{MnO}_3$ . By measuring the peak profile of Bragg reflections, upon cooling, we observed an increase in the width of the Bragg reflections around the Curie temperature (252 K) corresponding to the transition from a paramagnetic to a ferromagnetic state. Below approximately 200 K, dramatic changes in the width and integrated intensity were observed. Changes continued until the formation of charge ordering with  $q=(\frac{1}{2}, 0, 0)$  at  $T_{\text{CO}}=152$  K. This charge ordering was observed to be the first order transition with a large hysteresis width of 10 K. This sequent transition is understood by the formation of different magnetic domains at different temperature ranges as that observed by neutron powder diffraction. © 2008 American Institute of Physics.

[DOI: [10.1063/1.2957070](https://doi.org/10.1063/1.2957070)]

## I. INTRODUCTION

Studies of materials showing colossal magnetoresistance are at the frontier in solid-state physics due mainly to their potential for applications in memory devices and possible correlation with the related high- $T_C$  cuprate superconductors. Much effort has been devoted to the synthesis of manganites and the understanding of colossal magnetoresistance.<sup>1</sup> Typical manganite compounds are manganese oxides with the perovskite-type structure, such as  $R_{1-x}A_x\text{MnO}_3$  with  $R=\text{La, Pr, Bi, Nd}$  and  $A=\text{Sr, Ca}$ . Experiments have revealed a rich phase diagram with a variety of different structures as a function of stoichiometry, temperature, and applied magnetic field. These phases display a remarkable variety of magnetic properties caused by charge, spin, or orbital ordering. For instance, in the case of  $\text{Nd}_{1-x}\text{Sr}_x\text{MnO}_3$ ,<sup>2</sup> the compound undergoes a transition from a paramagnetic (PM) insulator to a ferromagnetic (FM) metal for  $x < 0.48$ , and from a PM insulator to a C-type antiferromagnetic (AFM) insulator for  $x > 0.63$ . For a hole concentration of  $0.48 < x < 0.52$ ,  $\text{Nd}_{1-x}\text{Sr}_x\text{MnO}_3$  first undergoes a transition to the FM metallic state at about 250 K, and then becomes an A-type AFM metal at about 200 K. Upon further cooling, it becomes a CE-type antiferromagnet at about 160 K, at which it has been reported to coexist with the A-type AFM state at low temperatures. The CE-type AFM state displays both charge and orbital ordering which are characterized by the alternate ordering of the  $\text{Mn}^{3+}$  and  $\text{Mn}^{4+}$  ions and by the ordering of  $d(3x^2-r^2)$  and  $d(3y^2-r^2)$  orbitals on the  $\text{Mn}^{3+}$  sites. The

unusual magnetic and electronic properties in these materials result from interaction between charge, spin, orbital, and lattice degrees of freedom, which are strongly coupled to each other.

$\text{Nd}_{0.5}\text{Sr}_{0.5}\text{MnO}_3$  shows a sequence of phase transitions from a PM insulator at high temperatures to a FM metal (Curie temperature  $T_C \approx 255$  K), and to an AFM insulator at  $T_{\text{CO}} \approx 158$  K.<sup>3</sup> As a generic feature of hole-doped perovskites of manganese oxides, the crystal undergoes a second-order transition from the state at Curie temperature ( $T_C$ ) via the double-exchange mechanism, and a first-order transition at  $T_{\text{CO}} (=T_N)$  from a metallic to an insulating state. This metal-insulator transition has been ascribed due mainly to the disproportional distortion of the  $\text{Mn}^{3+}$  and  $\text{Mn}^{4+}$  ions, to produce a charge-ordered AFM state, which collapses in an external magnetic field. A CE-type AFM structure with charge ordering has been observed below  $T_{\text{CO}}$  using neutron powder diffraction.<sup>2,4</sup> A dipole-resonance originating from the charge and orbital ordering was also reported by means of resonant x-ray scattering.<sup>5</sup> More recently, using neutron powder diffraction on  $\text{Nd}_{1/2}\text{Sr}_{1/2}\text{MnO}_3$ , Ritter *et al.*<sup>6</sup> observed the phase segregation that two different crystallographic structures and three magnetic phases coexist at low temperatures: orthorhombic (*Imma*) FM, orthorhombic (*Imma*) A-type AFM, and monoclinic ( $P2_1/m$ ) CE-type AFM phases. Also we note that for certain compounds of colossal magnetoresistance (CMR) materials, such as  $\text{La}_{1/2}\text{Ca}_{1/2}\text{MnO}_3$  and  $\text{Nd}_{1/2}\text{Sr}_{1/2}\text{MnO}_3$ , a spatially inhomogeneous distribution of domain structures has also been observed by Mori *et al.* and Fukumoto *et al.* using electron microscopy,<sup>7</sup> indicating a mixture of microdomain structures. Here, we report the experimental evidence, using high-

<sup>a)</sup>Electronic mail: [chd@mail.tku.edu.tw](mailto:chd@mail.tku.edu.tw).

<sup>b)</sup>Present address: Department of Physics, Shahrood University of Technology, Shahrood, Iran.

resolution x-ray scattering on a single crystal of  $\text{Nd}_{1/2}\text{Sr}_{1/2}\text{MnO}_3$ , to support these features of the phase segregation in CMR materials. A major distinction between our study and that of previous reports is that our observation of domain structures is observed in a single crystal rather than powder material. This has allowed us to determine the anisotropies in the domain sizes and in the correlation lengths, unencumbered by effects such as crystallite size and shape, endemic in studies of polycrystalline samples.

## II. EXPERIMENT AND DISCUSSION

A single crystal of  $\text{Nd}_{1/2}\text{Sr}_{1/2}\text{MnO}_3$  was cut from a boule grown by the standard floating zone method, and then polished to get a shiny and even surface with an area of  $\sim 2 \times 1 \text{ mm}^2$  using  $1 \mu\text{m}$  diamond paste. The lattice parameters  $a=5.431 \text{ \AA}$ ,  $b=7.625 \text{ \AA}$ , and  $c=5.477 \text{ \AA}$  with the space group of *Imma*(Ref. 8) were used for indexing the Bragg reflections. Preliminary measurements were carried out at the University of Durham using a four-circle triple-axis diffractometer on a rotating anode x-ray generator with a Cu target operated at 2.8 kW and a dispex closed-cycle cryostat. The longitudinal direction in the scattering plane was determined to be the  $\langle 1 \ 0 \ 1 \rangle$  direction. The alignment was completed by scanning many Bragg peaks, both in the scattering plane and out of the plane. The detailed studies utilizing synchrotron radiation were performed at station 16.3 at Daresbury Laboratory. A double bounce Si (1 1 1) monochromator was used to select the incident x-ray beam of  $1.000 \text{ \AA}$ , and a Si (1 1 1) single crystal was used as an analyzer. A solid state Ge detector with a narrow energy window was used to decrease the background scattering, including fluorescence and higher-order contamination.

A common feature of this crystal and many manganites with a high doping level is that of twinning. Typically the crystals are twinned in all three cubic directions of the underlying cubic perovskite structure. However such twins are macroscopic in size. In order to avoid probing the twin structure of the sample, a beam size of  $0.2 \times 0.1 \text{ mm}^2$  was used to search around the crystal until the Bragg reflections were found to be singlet. This technique ensures that although the sample may contain macroscopic twins, the volume of the crystal samples is overwhelmingly single domain. The mosaic width of the sample was determined to be  $\sim 0.05^\circ$  [full width at half maximum (FWHM)] as measured on the Bragg reflection (5, -2, 3) at room temperature. Such an experimental arrangement provides extremely high instrumental resolution and ensures that the widths of the Bragg reflections are entirely due to the size of coherent domains within the sample. The use of such a high-resolution analyzer ensures that even if more than one domain is illuminated by the x-ray beam the scattered radiation is only collected by the analyzer/detector from one domain. Others being slightly misaligned will not fulfill the Bragg condition of the analyzer. The relatively small rocking curve width of the crystal demonstrates the high quality of at least the part of the sample from which measurements were taken.

Using synchrotron x-ray scattering, we have demonstrated the existence of charge-ordering in  $\text{Nd}_{1/2}\text{Sr}_{1/2}\text{MnO}_3$  at

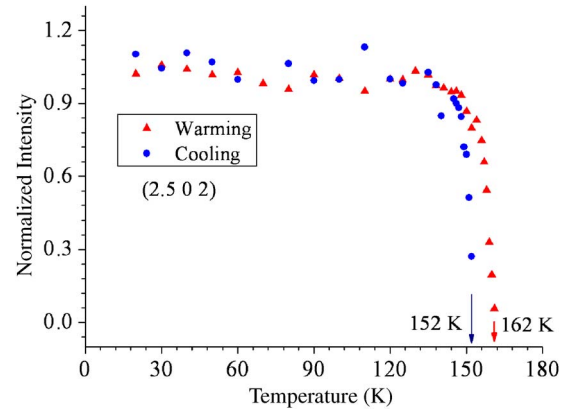


FIG. 1. (Color online) The evolution of the integrated intensities of the charge ordering reflection (2.5, 0, 2) as a function of temperature. There is an observed hysteresis width of about 10 K due to the first order phase transition.

low temperatures. The charge ordering was observed to double the unit cell along the  $a$  axis with a transition temperature of about 160 K upon warming. New satellite reflections are therefore observed at low temperatures with a wave vector of  $(\frac{1}{2} \ 0 \ 0)$ . These new charge-ordered satellite reflections have an intensity of about  $10^{-3}$  that of the principal Bragg reflections. Further studies confirmed that the transition temperature was  $T_{\text{CO}}=162 \text{ K}$ , and the transition belongs to the class of the first-order phase transition as observed by the transport measurements.<sup>2,3</sup> Thermodynamically, a general phenomenon associated with first-order transitions is the presence of hysteresis in cycling through the transition. Such a behavior is displayed in Fig. 1. It is clear that the charge ordering has different transition temperatures upon cooling and warming, i.e.,  $T_{\text{CO}}=152 \text{ K}$  for cooling and  $162 \text{ K}$  for warming, indicating the existence of hysteresis width of  $\sim 10 \text{ K}$  in agreement with the resistivity measurements.<sup>9</sup> Upon cooling the charge-ordered satellites were first observed at  $\sim 165 \text{ K}$ . At  $165 \text{ K}$ , they were very weak and broad, however, upon further cooling, they displayed a dramatic increase in intensity (see Fig. 3) and a corresponding spectacular decrease in width, as the crystallite regained long-range order.

As the charge-ordered state is characterized by a regular pattern of alternating valence states on Mn ions at  $T_{\text{CO}}$ , a structural phase transition is expected.<sup>2,6</sup> By carefully tracking the evolution of Bragg peaks around  $T_{\text{CO}}$ , we observed a transition region of about 1.3 K in where the high temperature phase coexists with the low temperature phase.<sup>10</sup> Such a first-order transition also reflects on the integrated intensity of the Bragg peaks above  $T_{\text{CO}}$ . The evolution of the integrated intensities of Bragg peak (5, -2, 3) as a function of temperature is displayed in Fig. 2. Upon cooling, the intensity of the Bragg peak first drops at  $T \approx 200 \text{ K}$ , and then a sharp and abrupt change takes place at  $T_{\text{CO}} \approx 152 \text{ K}$  because of the structural phase transition.<sup>6</sup> Similar behavior was also observed on warming run with a transition temperature of  $162 \text{ K}$ , and the intensity of the Bragg reflection reaching a maximum at about  $200 \text{ K}$ . The transition happened at  $T \approx 200 \text{ K}$ , upon cooling and warming runs, respectively, and is probably a second-order transition as the data shows no

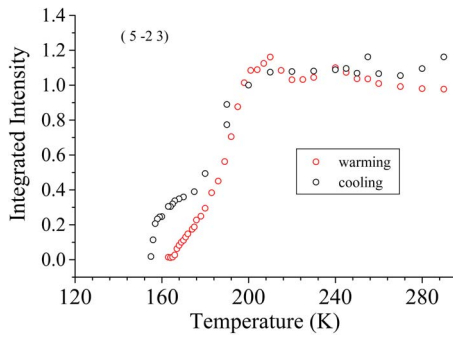


FIG. 2. (Color online) The evolution of the integrated intensities of the Bragg reflection (5, -2, 3) as a function of temperature. There is an observed hysteresis width of about 10 K due to the first order phase transition.

hysteresis. In Fig. 2, it is also noteworthy that both curves measured in cooling and warming runs split at  $T \approx 180$  K, suggesting the existence of a nonequilibrium state between domains in the temperature range 180–160 K due to the first order phase transition at  $T_{CO}$ . Using neutron powder diffraction, Kajimoto *et al.* reported that  $\text{Nd}_{1-x}\text{Sr}_x\text{MnO}_3$  with  $x \approx 0.5$  undergoes a structural phase transition from a FM phase to an A-type AFM phase at  $T \approx 200$  K.<sup>2</sup> As x rays are not sensitive to changes of magnetic phases but to the changes of domain sizes in a crystal, the decrease in the integrated intensities of Bragg peak, as shown in Fig. 2, suggests that the FM domains break into smaller domains at  $T \approx 200$  K due to the formation of A-type AFM domains.

The suggestion of a change in the size of the domains is also supported by measurements of the Bragg peak width along the longitudinal direction as displayed in Fig. 3. It is clear that both curves, measured upon cooling and warming runs, split at  $T \approx 180$  K. Below 180 K, the peak widths diverge as the temperature approaches  $T_{CO}$ , indicating a decrease of the length scale of the long-range ordered structure. A structural phase transition occurs at  $T_{CO} \approx 152$  K due to the different valence states of the Mn ions, resulting in the formation of the charge ordered state. Again, this splitting can be ascribed to the hysteresis behavior due to the first-order phase transition at  $T_{CO}$ .<sup>6</sup>  $\text{Nd}_{1/2}\text{Sr}_{1/2}\text{MnO}_3$  is a PM insulator at room temperature and undergoes a transition to a FM metallic state at  $T \approx 248$  K.<sup>2,4</sup> By measuring the evolu-

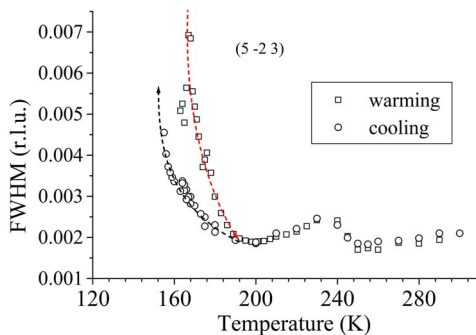


FIG. 3. (Color online) Scans through the longitudinal direction of the Bragg peak (5, -2, 3) displaying changes of the peak width (FWHM) with temperature on cooling and warming. The splitting at  $T \approx 180$  K can be ascribed to the hysteresis behavior due to the first order phase transition at  $T_{CO}$ , and the peak broadening around  $T \approx 238$  K to the mixture of domains.

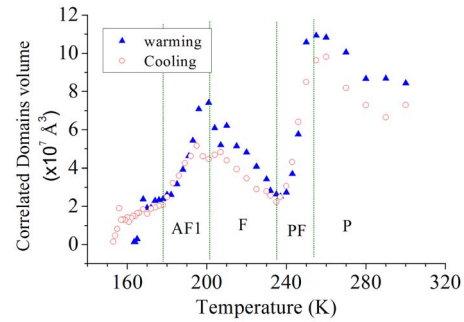


FIG. 4. (Color online) Temperature dependence of the correlated domain sizes. Data were extracted from scans through the  $H$ ,  $K$ , and  $L$  directions of the Bragg peak (5, -2, 3). The evolution can be roughly divided into the regimes of the P (PM state), PF (a mixture of PM and FM states), F (FM state), and AF1 (a mixture of AFM and FM states).

tion of the peak width with temperature, our data are in agreement with the studies of the transport and neutron powder diffraction measurements. As shown in Fig. 3, the width of the Bragg reflection shows unusual peak broadening around the transitions from PM to FM and FM to AFM charge-ordered phases. Such a broadening of the Bragg peak was also observed by Radaelli *et al.*<sup>11</sup> in  $\text{La}_{1/2}\text{Ca}_{1/2}\text{MnO}_3$ . The peak width increases at  $T \approx 252$  K and then decreased at  $T \approx 234$  K, indicating a transition starting at 252 K, which is completed at 234 K. In the PM state, magnetic domains distribute randomly, but align ferromagnetically in the FM state. Such a picture is consistent with our measured data. Starting from high temperature, the peak profile became sharp as the temperature was lowered, indicating that the randomly distributed domains tended to become ordered and correlated over a longer distance. At 252 K, the domains start to break up into smaller domains due to the formation of the FM phase, as demonstrated by an abrupt change in both resistivity and magnetization.<sup>3</sup> This change is continuous, and it suggests the existence of a mixture of both domains, PM and FM domains, in the temperature range 252–234 K. The PM state disappeared below 234 K. Such a transition has been reported by both transport and neutron powder diffraction measurements.<sup>2,4,6</sup>

In order to further study the evolution of the domain structures with temperature, we also performed scans along the three crystallographic axes,  $H$ ,  $K$ , and  $L$ , individually. The corresponding structural correlation lengths were obtained from  $\xi = 1/\delta(2\pi/a)$ , where  $\delta$  is the half width at half maximum (HWHM) and  $a$  the lattice parameter. The correlated domain volume was determined from the product of the three correlation lengths that were calculated from the widths (HWHMs) of the Bragg peak (5, -2, 3) along the  $H$ ,  $K$ , and  $L$  directions and is displayed in Fig. 4. We realize that this determined domain size may not be the actual size of the domains,<sup>12</sup> but rather the size of long-range correlations within a crystallite. However, it will reflect the domain structure, size, and dislocation density and the effect of magnetic and crystallographic transitions. For temperatures above 252 K, (the region marked P in Fig. 4), the PM domains were observed to grow as the temperature was lowered, indicating that the long-range order was forming. Upon cooling, we observed a drop of about 70% in the volume of the correlated

domains from 252 to 234 K, as shown the region marked PF in Fig. 4. As explained above, this is due to the transition of the PM state to the FM state. In the interval 234–200 K, the size of the domains increases with decreasing temperature and the integrated intensities increase as well. The development of a long-range order of the FM state stops at about 200 K, where the integrated intensity starts to drop and the peak profiles became increasingly broad upon cooling as shown in Figs. 2 and 3. An A-type AFM phase in which the spins of Mn ions antiferromagnetically order along the  $b$  axis with a  $d_{x^2-y^2}$  orbital ordering has been demonstrated to coexist with a FM phase below 200 K on neutron powder diffraction patterns.<sup>2,6</sup> Using transmission electron microscopy, Fukumoto *et al.* also observed the transformation of microstructures relating to the microscopic-scale electronic phase separation.<sup>7</sup> Upon further cooling, a turning point on the transition curves of Fig. 4 was observed at  $T \approx 182$  K. Such a discontinuous change is more pronounced on the curves along the  $H$  and  $L$  directions than that along the  $K$  direction. The origin of this is not exactly known yet, but it might be the precursor of orbital ordering. It has been demonstrated that orbital ordering results from a cooperative Jahn–Teller effect distorting the  $M^{3+}O_6$  octahedra, associated with long Mn<sup>3+</sup>-O bonds along the  $a$  and  $c$  axes, which could suppress the domains formed at high temperatures and change the distribution of domains. Kajimoto *et al.* proposed that orbital ordering could cause the observed phase segregation,<sup>2</sup> and therefore it could explain the coexistence of the CE- and A-type AFM phases at low temperatures. Kajimoto *et al.*<sup>13</sup> observed a two-component feature at around the FM transition temperature  $T \approx 250$  K in a single crystal of Nd<sub>1/2</sub>Sr<sub>1/2</sub>MnO<sub>3</sub> using inelastic neutron scattering. Between the two components, the central component was observed to be the quasielastic scattering originated from the PM phase and persist even in the FM state, suggesting the coexistence of PM and FM phases below 250 K. This finding supports our explanation for the changes of the peak profiles in the temperature range from about 230 to 250 K. The coexistence of multiple phases ascribed to microdomain structures in the temperature range of  $T_N < T < T_C$  was also observed in Pr<sub>1/2</sub>Ca<sub>1/2</sub>MnO<sub>3</sub>, Nd<sub>1/2</sub>Sr<sub>1/2</sub>MnO<sub>3</sub>, and La<sub>1/2</sub>Ca<sub>1/2</sub>MnO<sub>3</sub> using electron microscopy and neutron diffraction on powder samples.<sup>6,7,14</sup> Upon further cooling, a transition occurred at  $T_{CO} \approx 152$  K, which is in accord with the formation of the CE-type charge/spin ordering. Measurements were also taken on the warming run, showing the identical behavior except for the different transition temperature ( $\approx 162$  K) for the disappearance of the charge ordering due to the first order phase transition.<sup>15</sup>

### III. CONCLUSION

We have reported the transformation of domain structures and the formation of charge ordering in *single crystal* Nd<sub>1/2</sub>Sr<sub>1/2</sub>MnO<sub>3</sub> using synchrotron x-ray scattering. Nd<sub>1/2</sub>Sr<sub>1/2</sub>MnO<sub>3</sub> is orthorhombic with a space group of *Imma* at room temperature and does not undergo a structural transition until  $T_{CO}$  where the charge ordered AFM state forms. The phase transitions observed in the temperature interval

( $T_{CO} < T < 200$  K) are unlikely to be caused by the structural phase transition. Instead, it is evidence for phase segregation due to the formation of different magnetic domains. Such a mixture of magnetic phases has previously been observed in powdered material using neutron powder diffraction. Our study demonstrates that such effects can also be observed in a bulk single crystal using high resolution synchrotron x-ray scattering. As Nd<sub>1/2</sub>Sr<sub>1/2</sub>MnO<sub>3</sub> is a typical charge ordered CMR material, the application of a magnetic field can significantly change the magnetic states. The observed phase segregation, especially in the temperature range of  $T_{CO} < T < 200$  K, could therefore also be sensitive to the application of magnetic field.<sup>14</sup>

### ACKNOWLEDGMENT

This paper was supported by a grant from the Engineering and Physical Sciences Research Council. One of the authors (M.E.G.) thanks the Ministry of Science, Research, and Technology of Iran for financial support for his doctoral studies. Work at Rutgers was supported by NSF-DMR-0520471. C.H.D. is thankful for the grant support from the National Science Council, Taiwan, under the NSCT Grant No. 96-2112-M-032-009-MY3.

<sup>1</sup>For reviews, see, S.-W. Cheong and C. H. Chen, ‘Stripe, Charge & Orbital Ordering in Perovskite Manganites’, in *Colossal Magnetoresistance and Related Properties* edited by B. Raveau and C. N. R. Rao (World Scientific, Singapore); and *Colossal Magnetoresistance Oxides* edited by Y. Tokura & Breach, London, 1999).

<sup>2</sup>R. Kajimoto, H. Yoshizawa, H. Kawano, H. Kuwahara, Y. Tokura, K. Ohoyama, and M. Ohashi, *Phys. Rev. B* **60**, 9506 (1999).

<sup>3</sup>H. Kuwahara, Y. Tomioka, A. Asamitsu, Y. Moritomo, and Y. Tokura, *Science* **270**, 961 (1995).

<sup>4</sup>H. Kawano, R. Kajimoto, H. Yoshizawa, Y. Tomioka, H. Kuwahara, and Y. Tokura, *Phys. Rev. Lett.* **78**, 4253 (1997).

<sup>5</sup>K. Nakamura, T. Arima, A. Nakazawa, Y. Wakabayashi, and Y. Murakami, *Phys. Rev. B* **60**, 2425 (1999).

<sup>6</sup>C. Ritter, R. Mahendiran, M. R. Ibarra, L. Morellon, A. Maignan, B. Raveau, and C. N. R. Rao, *Phys. Rev. B* **61**, R9229 (2000).

<sup>7</sup>S. Mori, C. H. Chen, and S.-W. Cheong, *Phys. Rev. Lett.* **81**, 3972 (1998); N. Fukumoto, S. Mori, N. Yamamoto, Y. Moritomo, T. Katsufuji, C. H. Chen, and S.-W. Cheong, *Phys. Rev. B* **60**, 12963 (1999).

<sup>8</sup>V. Caignaert, F. Millange, M. Hervieu, E. Suard, and B. Raveau, *Solid State Commun.* **99**, 173 (1996); P. M. Woodward, T. Vogt, D. E. Cox, C. N. R. Rao, and A. K. Cheetham, *Chem. Mater.* **11**, 3528 (1999).

<sup>9</sup>Y. Tokura, H. Kuwahara, Y. Moritomo, Y. Tomioka, and A. Asamitsu, *Phys. Rev. Lett.* **76**, 3184 (1996).

<sup>10</sup>C.-H. Du, Y. Su, M. E. Ghazi, P. D. Hatton, S. P. Collins, S. Brown, and S.-W. Cheong, *published in Magnetic and Superconducting Materials (MSM-99)* edited by M. Akhavan, J. Jensen, and K. Kitazawa (World Scientific Press, London, 2000), pp. 936–942.

<sup>11</sup>P. G. Radaelli, D. E. Cox, M. Marezio, and S.-W. Cheong, *Phys. Rev. B* **55**, 3015 (1997).

<sup>12</sup>Strictly speaking, in order to obtain the actual correlated domain size the peak profiles should be deconvoluted from the resolution function. In this study, our resolution function was so very narrow compared to the measured Bragg widths that such a deconvolution is unnecessary.

<sup>13</sup>R. Kajimoto, H. Yoshizawa, H. Kawano, H. Kuwahara, and Y. Tokura, *J. Phys. Chem. Solids* **60**, 1177 (1999); H. Kawano, R. Kajimoto, H. Yoshizawa, Y. Tomioka, H. Kuwahara, and Y. Tokura, *Phys. Rev. Lett.* **78**, 4254 (1997); R. Kajimoto, T. Kakeshita, Y. Oohara, H. Yoshizawa, Y. Tomioka, and Y. Tokura, *Phys. Rev. B* **58**, R11837 (1998).

<sup>14</sup>C. H. Chen and S.-W. Cheong, *Phys. Rev. Lett.* **76**, 4042 (1996); S. Mori, T. Katsufuji, N. Yamamoto, C. H. Chen, and S.-W. Cheong, *Phys. Rev. B* **59**, 13573 (1999).

<sup>15</sup>S. Shimomura, K. Tajima, N. Wakabayashi, S. Kobayashi, H. Kuwahara, and Y. Tokura, *J. Phys. Soc. Jpn.* **68**, 1943 (1999).